Spherically-symmetric mass accretion onto logatropic protostars

L. Di G. Sigalotti
Centro de Física, Instituto Venezolano de Investigaciones Científicas, IVIC, Apartado 21827, Caracas 1020A, Venezuela

Recibido el 25 de noviembre de 2003; aceptado el 22 de febrero de 2004

We follow the spherical gravitational collapse and the subsequent accretion phase of nonsingular $A = 0.2$ logatropes of both subcritical and critical masses using numerical hydrodynamics. The initial configuration is close to hydrostatic equilibrium. In all cases, we assume fiducial values of the central temperature ($T_c = 10$ K) and surface pressure ($p_{\rm s}/k = 1.3 \times 10^5$ cm^{-3} K) that are appropriate for star formation in isolated environments. We find that immediately after the transition toward a singular density profile, the mass accretion rate increases abruptly in a very short timescale followed by a phase of much slower increase, after which a peak value of $\dot{M}_{\rm acc}$ is reached. At this point about 40% of total mass has been accreted by the central protostar. Thereafter, the accretion rate declines for the remainder of the evolution until 100% of the total core mass is condensed into a form of stellar mass. The results predict peak values of $\dot{M}_{\rm acc}$ as high as $\sim 5 - 6 \times 10^{-5}\ M_\odot$ yr^{-1} for logatropes close to the critical mass and imply that stars of mass $1\ M_\odot \leq\ M_\star \leq 92\ M_\odot$ all form within 3.6–6.6×10^6 years. The models are representative of the early protostellar phase from Class 0 to Class I objects.

Keywords: Hydrodynamics; star formation; accretion and accretion disks.

Haciendo uso de un código hidrodinámico se calcula el colapso gravitacional y la acreción de esferas logatrópicas no-singulares con $A = 0.2$ y masas subcríticas y crítica, a partir de configuraciones cercanas al equilibrio hidrostático. Para todos los modelos se toman valores de la temperatura central ($T_c = 10$ K) y de la presión superficial externa ($p_{\rm s}/k = 1.3 \times 10^5$ cm^{-3} K) consistentes con los valores típicos en regiones donde la formación estelar ocurre en forma aislada. Inmediatamente después que la esfera alcanza un perfil singular de densidad, la tasa de acreción aumenta abruptamente en una escala de tiempo muy corta. A esta fase sigue una de crecimiento más lento en la cual $\dot{M}_{\rm acc}$ aumenta hasta alcanzar un máximo valor. A este punto de la evolución cerca del 40% de la masa total ha sido acrecida por la protoestrella. Luego la tasa de acreción decrece lenta y progresivamente por el resto de la evolución hasta que el 100% de la masa total es convertida en masa estelar. Los resultados predicen valores máximos de $\dot{M}_{\rm acc}$ del orden de $\sim 5 - 6 \times 10^{-5}\ M_\odot$ yr^{-1} para logatropos con masa cercana al valor crítico e indican que estrellas con masas entre 1 y $92\ M_\odot$ se forman en 3.6–6.6×10^6 años. Los modelos se aplican a la fase de evolución protoestelar comprendida entre objetos de la Clase 0 y I.

Descriptores: Hidrodinámica; formación estelar; acreción y discos de acreción

PACS: Hidrodinámica; Formación estelar; Acreción y discos de acreción

1. Introduction

Over the past few years our understanding of star formation has notably improved both theoretically and observationally. However, the precise way in which dense molecular cloud cores, i.e., the condensations that form at scales less than a parsec within large molecular clouds [1,2], condense to form stellar objects is still unclear.

Observations of the internal structure of both low- and high-mass dense cores are essential constrain the initial conditions for current star formation models. For instance, many theoretical models of star forming clouds employ the singular isothermal sphere, in which $\rho \propto r^{-2}$ [3]. However, this model is not applicable to more realistic clouds with finite central densities such as the marginally stable Bonnor-Ebert sphere. In particular, numerical hydrodynamic calculations of the isothermal collapse of critically stable Bonnor-Ebert spheres predict that 44% of the mass infalls at a few times the speed of sound once a central protostellar core has formed [4]. Although recent observations indicate that some starless cloud cores can be very well fitted by the structure of pressure-bounded Bonnor-Ebert spheres [5,6], there is complete lack of evidence in support of such high collapse velocities. Moreover, it is also well-known on observational grounds that the nonthermal component $\sigma_{\rm NT}$ of the total velocity dispersion dominates over the thermal one in massive cores [7]. In addition, significant nonthermal motion has also been detected in low-mass cores [7,8]. In particular, the nonthermal line widths in the former cores are consistent with $\sigma_{\rm NT} \propto r^{0.21}$, while $\sigma_{\rm NT} \propto r^{0.53}$ in the latter ones [7], implying that the velocity dispersion rises more steeply with the radius in low-mass cores than in massive ones. Since $\sigma_{\rm NT}$ is observed to decrease toward small radii inside molecular clouds and within individual dense cores [7]. This decrease suggests that nonthermal support must come largely from magnetohydrodynamic (MHD) turbulence on the largest scales and that velocities are in prevalence of thermal origin at the smallest scales. Evidently, these properties cannot be accounted for with the use of a simple isothermal equation of state.

Alternatively, McLaughlin and Pudritz [9] introduced a logatropic equation of state in which the nonthermal (turbulent) effects are modelled through a logarithmic dependence of the pressure on density. They showed that this form reproduces on average the observed internal velocity-dispersion of both molecular clouds and cores of low and high mass. In a separate paper [10], these authors derived solutions for both the equilibrium and self-similar collapse of logatropic

spheres. In particular, the unstable singular equilibrium with $\rho \propto r^{-1}$ everywhere is the analogy for Shu's [3] unstable singular isothermal sphere, whereas the stable nonsingular equilibrium solution is the counterpart of the hydrostatic Bonnor-Ebert sphere. Recently, Reid *et al.* [11] performed fully three-dimensional hydrodynamic simulations of the gravitational collapse of nonsingular spherical logatropes of fiducial mass $< 5\ M_\odot$. These calculations were extended to much higher masses (up to the critical value) by Sigalotti et al. [12], who found that about 6% of the mass collapses supersonically in a $1\ M_\odot$ sphere, while only $\sim 0.02\%$ behaves in this manner in a critical ($\approx 92.05\ M_\odot$) logatrope. This finding is in clear contrast with the 44% prediction for the collapse of the critically stable Bonnor-Ebert sphere [4]. In this paper, we shall follow the mass accretion history of isolated logatropes of varied masses up to the point where 100% of the total mass has been accreted by the central protostar and compare the results with observational estimates for Class 0 and Class I objects.

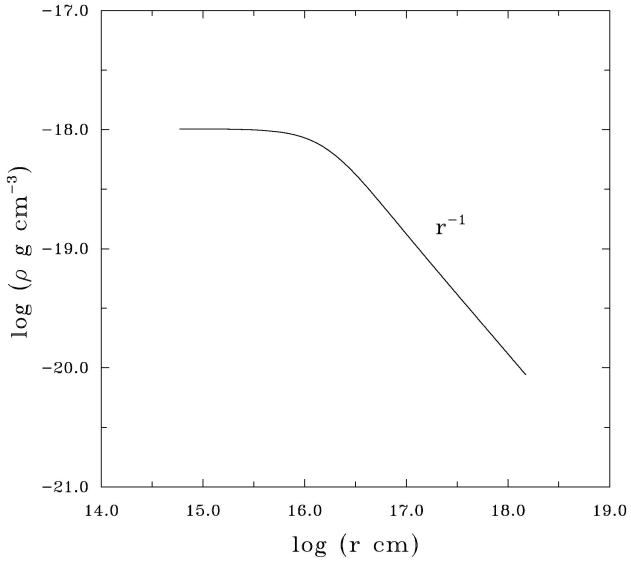

FIGURE 1. Nonsingular density profile of a pressure-truncated, $A = 0.2$ logatrope of critical mass $M \approx 92.05\ M_\odot$.

2. Initial Conditions

We define a sequence of seven model calculations of nonsingular logatropes of both subcritical (1, 10, 50, 60, 80 and 90 $M_\odot$) and critical ($\approx 92.05\ M_\odot$) masses, all starting with a central temperature of 10 K and a fiducial truncation pressure $p_s/k = 1.3 \times 10^5$ cm^{-3} K. With this choice of the parameters the models are appropriate for isolated star formation. The stable nonsingular equilibria from which the calculations start are constructed as described in Ref. 12, using the logatropic equation of state [9,10]

$$p = p_c \left[1 + A \ln\left(\frac{\rho}{\rho_c}\right)\right] , \qquad (1)$$

where p_c and ρ_c refer to central values and $A = 0.2$, which gives the best fit of Eq. (1) to the observed internal velocity-dispersion profiles for low- and high-mass cores [9].

The nonsingular density profile for the critically stable ($\approx 92.05\ M_\odot$) logatrope is shown in Fig. 1. Similar variations are obtained for all other subcritical spheres. We see that the cloud is singular with $\rho \propto r^{-1}$ in the outer layers. The collapse of the nonsingular spheres is initiated by adding a 5% density enhancement to the equilibrium profile at all radii. For the details of this initial collapse phase, we refer the reader to [12]. This phase ends when the entire cloud approaches a singular density profile everywhere at time $t = 0$. In particular, near the center an $r^{-3/2}$ density profile sets in, which extends in radius up to $r = r_0$, where $r_0 = 3\sigma_c/(4\pi G\rho_c)^{1/2}$ is the characteristic radius of the spherical core. Here $\sigma_c^2 = p_c/\rho_c$ is the central velocity dispersion. For $r > r_0$, the profile matches the $\rho \propto r^{-1}$ power-law. Recent observational evidence indicates power-law density variations in the structure of Class 0 objects that match the density profiles of both equilibrium ($\rho \propto r^{-1}$) and collapsing ($\rho \propto r^{-3/2}$) logatropic spheres [13]. Similar evidence has also been found for the structure of young massive stars [14].

The calculations of this paper were performed using a 1D hydrodynamics code based on a second-order accurate Lagrangian remap technique. Temporal second-order accuracy is enforced by solving the Lagrangian equations in a predictor-corrector fashion. After the Lagrangian update, the solution is mapped back onto a Eulerian grid that is allowed to follow as close as possible the Lagrangian motion. The initial collapse phase is calculated using only the Lagrangian version of the code to guarantee sufficient spatial resolution near the origin $r = 0$. At the precise time of singularity formation, the smallest central grid shells are lopped off into a sink cell in order to remove from the calculation the details of the flow around the singularity. An inflow/outflow boundary condition is implemented across the sink cell surface. Once the sink cell is activated, the subsequent evolution is calculated using the Eulerian version of the code. In this way, the mass which enters the sink is assumed to be condensed into a central point mass located at the origin. This mass ($M_{\rm acc}$) will no longer interact hydrodynamically with the rest of the grid, but only gravitationally via a point mass potential. The outer core surface is handled by keeping the pressure there at a constant value equal to the truncation pressure p_s. A more detailed account of the methods, sink cell treatment and boundary conditions is given in [12]. In contrast with those previous calculations, we use here an increased initial spatial resolution consisting of 400 uniformly distributed radial zones.

3. Logatropic Accretion Phase

In this section, we describe the evolution starting from the time ($t = 0$) of singularity formation and monitor the tempo-

ral variation of $M_{\rm acc}(t)$ only when the sink cell is activated ($t > 0$). The details of the mass accretion history for all models considered is displayed in Fig. 2, where the central mass accretion in solar masses (Fig. 2a) and the central mass accretion rate in units of solar masses per year (Fig. 2b) are shown as functions of time. In all cases, the evolution is followed up to the point where 100% of the total mass has been accreted by the growing central protostar. We see from Fig. 2a that the accretion lifetime increases with increasing mass up to $50\ M_\odot$ and then decreases as the mass approaches its critical limit, implying that stars of mass between 1 and $\approx 92.05\ M_\odot$ all form within 3.6–6.6×10^6 yr. The weak dependence of the free-fall time on mass and the initial t^4 dependence of the mass accretion in logatropes [10], are responsible for this small spread in the star-formation times. Immediately after singularity formation, the mass accretion rate grows steeply in a very short timescale (Fig. 2b). This feature is common to all masses. This phase is followed by one of much slower increase which ends when a maximum value of $\dot{M}_{\rm acc}$ is achieved, corresponding to the point where about 40% of the total available mass has been accreted by the central protostar. We also note that the higher the total core mass, the steeper the growth of the accretion rate during this intermediate phase. In particular, the present models predict peak values of $\dot{M}_{\rm acc}$ between $\sim 8 \times 10^{-7}\ M_\odot$ yr^{-1} for a $1\ M_\odot$ core and $\sim 6 \times 10^{-5}\ M_\odot$ yr^{-1} for a critical logatrope. Thereafter, the accretion rate decreases steadily for the remainder of the evolution. Such a decline is expected because the central protostar is drawing mass from a finite reservoir. Once the expansion wave reaches the outer boundary, it will not set new mass into collapse and so the flow of inward-moving material cannot be maintained at the same rate.

These models are suggestive of the early phases of protostellar evolution, including the Class 0 stage, in which the protostar contains half the mass of the initial core [15], and the Class I stage, in which the protostar accretes the remainder of the final stellar mass, leading to the formation of an optically visible young star (Class II object). In our models, the transition from a nonsingular to a singular collapse (when a central point-mass forms) marks the beginning of the Class 0 stage. The calculations predict lifetimes for this phase of $\sim$ 1.5–5.3×10^5 yr, consistent with the observational estimates of a few 10^5 yr reported by Gregersen and Evans [16] for a sample of collapsing sources representative of Class 0 objects. Furthermore, the logatropic models predict timescales of $\sim$ 0.7–1.6×10^6 yr for the transition from Class 0 to Class I sources and of $\sim$ 2.9–5×10^6 yr from Class I to Class II objects. This implies predicted lifetimes of $\sim$ 0.8–1.0×10^6 yr for the Class 0 phase and of $\sim$ 2.0–3.5×10^6 yr for the Class I phase. Observational estimates suggest a Class 0 lifetime of $\sim$ 1–3×10^4 yr compared to $\sim 2 \times 10^5$ yr for the Class I sources in the ρ Oph main cloud [17]. These times are $\sim$ 1–2 orders of magnitude shorter than those predicted by the present logatropic models. However, these estimates refer to regions of multiple star formation,

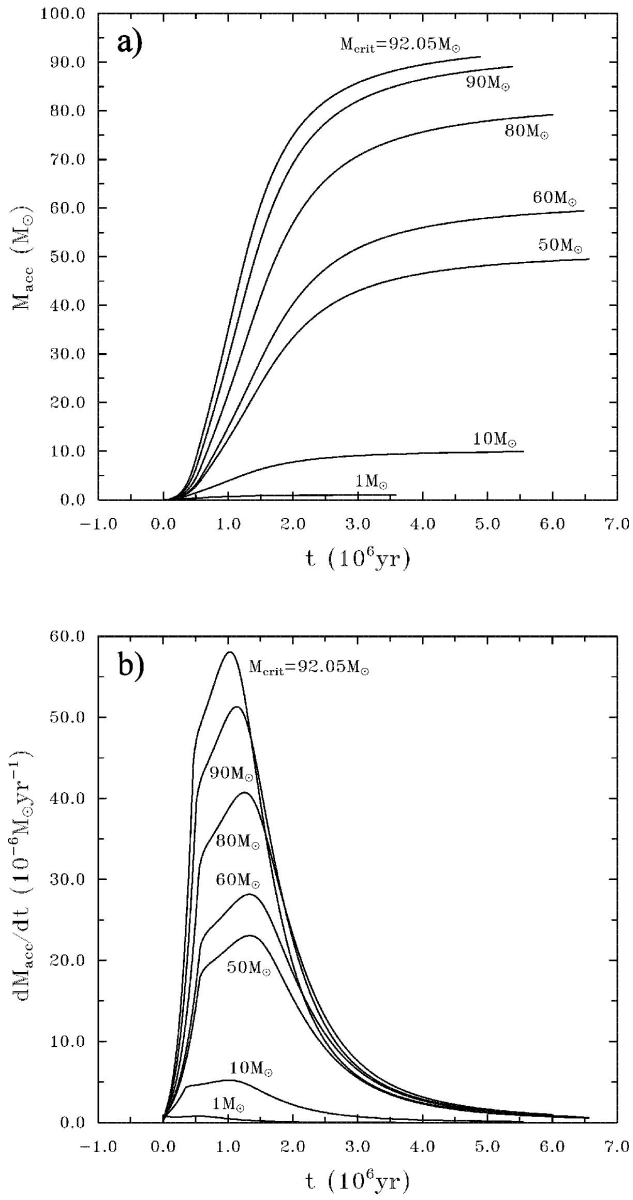

FIGURE 2. a) Temporal evolution of the central mass accretion and b) central mass accretion rate in physical units for all logatropic core masses considered. The evolution is shown up to the point where nearly all of the finite core mass has fallen into the central protostar.

while the present models apply to isolated star-forming regions. In addition, the transition from Class 0/I to Class I/II has been determined by assuming that there are no disruption mechanisms operating during protostellar evolution and that the final stellar mass is determined by the total core mass, which has no observational support. In particular, there is strong evidence that outflows are directly powered by mass accretion and that their decline is correlated to a corresponding decline of the mass accretion rate during the evolution from the Class 0 to the Class I stage [18].

At the borderlines indicative of the transition between Class 0 and Class I sources, the logatropic models predict $\dot{M}_{\rm acc}\sim 0.07$–$5.5\times10^{-5}\ M_\odot$ yr^{-1}. The corresponding values for the transition between Class I and Class II protostars are $\dot{M}_{\rm acc}\sim 0.02$–$1.4\times10^{-6}\ M_\odot$ yr^{-1}. These values are consistent with the inferred decrease from ~ 0.3–$1\times10^{-5}\ M_\odot$ yr^{-1} for Class 0 sources to ~ 0.7–$2\times10^{-7}\ M_\odot$ yr^{-1} for evolved Class I protostars [19]. Further recent estimates for massive protostars indicate accretion rates $\geq 10^{-5}\ M_\odot$ yr^{-1} [20], which agree with our predicted Class 0 lifetimes for high-mass ($\geq 50\ M_\odot$) logatropes. Because of the high luminosities of young massive stars, radiative acceleration may significantly contribute to the dynamical evolution of high-mass cores, leading to larger sizes of the accretion rate, shorter lifetimes and smaller final stellar masses than predicted by the present hydrodynamic collapse models. A further step towards improving the picture of logatropic collapse is the inclusion of rotation. In this case, anisotropic accretion throughout the formation of a flattened circumstellar disk is likely to affect the spherically symmetric timescales and accretion rates predicted here, which may still apply to the limiting case of very slow rotation.

1. R. Chini *et al.*, *Astrophys. J.* **474** (1997) L135.
2. T.L. Wilson, R. Mauesberger, P.D. Gensheimer, D. Muders and J. H. Bieging, *Astrophys. J.* **525** (1999) 343.
3. F.H. Shu, *Astrophys. J.* **214** (1977) 488.
4. P.N. Foster and R.A. Chevalier, *Astrophys. J.* **416** (1993) 303.
5. A. Bacmann *et al.*, *Astron. Astrophys.* **361** (2000) 555.
6. J.F. Alves, C.J. Lada and E.A. Lada, *Nature* **409** (2001) 159.
7. P. Caselli and P.C. Myers, *Astrophys. J.* **446** (1995) 665.
8. G.A. Fuller and P.C. Myers, *Astrophys. J.* **384** (1992) 523.
9. D.E. McLaughlin and R.E. Pudritz, *Astrophys. J.* **469** (1996) 194.
10. D.E. McLaughlin and R.E. Pudritz, *Astrophys. J.* **476** (1997) 750.
11. M.A. Reid, R.E. Pudritz and J. Wadsley, *Astrophys. J.* **570** (2002) 231.
12. L. Di G. Sigalotti, F. de Felice and E. Sira, *Astron. Astrophys.* **395** (2002) 321.
13. C.J. Chandler and J.S. Richer, *Astrophys. J.* **530** (2000) 851.
14. F.F.S. van der Tak, E.F. van Dishoeck, N.J. II Evans and G.A. Blake, *Astrophys. J.* **537** (2000) 283.
15. P. André, D. Ward-Thompson and M. Barsony, *Astrophys. J.* **406** (1993) 122.
16. E.M. Gregersen and N.J. Evans, *Astrophys. J.* **538** (2000) 260.
17. T.P. Greene, B.A. Wilking, P. André, E. T. Young and C. J. Lada, *Astrophys. J.* **434** (1994) 614.
18. S. Bontemps, P. André, S. Terebey and S. Cabrit, *Astron. Astrophys.* **311** (1996) 858.
19. P. André, D. Ward-Thompson and M. Barsony, in Protostars and Planets IV, Eds. V. G. Mannings, A. P. Boss and S. S. Russell, Tucson: Univ. Arizona Press (2000) 59.
20. J.A. Eisner, L.J. Greenhill, J.R. Herrnstein, J.M. Moran and K.M. Menten, *Astrophys. J.* **569** (2002) 334.